BJRS

BRAZILIAN JOURNAL
OF
RADIATION SCIENCES
11-01A (2023) | 01-17 | e2157

Exposure computational models with voxel phantoms coupled to EGSnrc Monte Carlo code

Vieira[a,b], J. W.; Leal Neto[a], V.; Andrade[a], P. H. A.; Oliveira[a,e,f], A. C. H.; Lima[d], V. J. M.; Lacerda[e,g], I. V. B.; Bezerra[a], L. R. A.; Silva[e], A. N. C.; Santos[h], W. S.; Santana[c], I. E.; Farias[c], W. A. W. A.; Santos[c], L. C. S.; Oliveira[1] F. G.; Lima[c,f], F. R. A.

[a]*Instituto Federal de Educação, Ciência e Tecnologia de Pernambuco, IFPE, 50740-540, Recife, Brasil*
[b]*Escola Politécnica de Pernambuco-UPE, 50750-470, Recife, PE, Brasil*
[c]*Departamento de Energia Nuclear-UFPE, 50740-540, Recife, PE, Brasil*
[d]*Departamento de Anatomia-UFPE, 50670-901, Recife, PE, Brasil*
[e]*Departamento de Física-UFPE, 50760-901, Recife, PE, Brasil*
[f]*Centro Regional de Ciências Nucleares-CRCN-NE/CNEN, 50740-540, Recife, PE*
[g]*Faculdade Nova Esperança, FACENE-FAMENE, 58067-695, João Pessoa, PB, Brasil*
[h]*Instituto de Física, Universidade Federal de Uberlândia, 38408-100, Uberlândia, MG, Brasil*
jose.wilson@recife.ifpe.edu.br

ABSTRACT

In computational dosimetry of ionizing radiation, the energy deposited in radiosensitive organs and tissues is evaluated when an anthropomorphic simulator (phantom) is irradiated using Exposure Computational Models (ECMs). An ECM is a virtual scene with a phantom positioned mathematically relative to a radioactive source. The initial state includes information like the type of primary particle, its energy, starting point coordinates, and direction. Subsequently, robust Monte Carlo (MC) codes are used to simulate the particle's mean free path, interaction with the medium's atoms, and energy deposition. These are common steps for simulations involving photons and/or primary electrons. The GDN (Research Group on Numerical Dosimetry and the Research Group on Computational Dosimetry and Embedded Systems) has published ECMs with voxel phantoms irradiated by photons using the MC code EGSnrc. This work has led to specific computational tools development for various numerical dosimetry stages, including input file preparation, ECM execution, and result analysis. Since 2004, the GDN developed in-house applications like FANTOMAS, CALDose_X, DIP, and MonteCarlo. Certain previously used phantoms are reintroduced to provide historical context in the ECMs' production timeline, emphasizing additive modifications inherent in systematic theme studies. The dosimetric evaluations used the binary version of the MASH (Male Adult mesh) phantom, converted to the SID (Dosimetric Information System) text file type. This format has been used by the group since 2021 to couple a voxel phantom to the EGSnrc user code. The ECM included an environmental dosimetry problem simulation. Most of these tools are accessible on the GDN page (http://dosimetrianumerica.org).

Keywords: Exposure Computational Models, voxel phantoms, Monte Carlo, EGSnrc.

ISSN: 2319-0612
DOI: https://doi.org/10.15392/2319-0612.2023.2157
Submitted: 2022-11-25
Accepted: 2023-10-02

1. INTRODUCTION

Producing the distribution of energy deposited into the regions of interest of an irradiated body requires specific phantoms coupled to computational systems containing robust MC codes and validated radioactive source simulator algorithms. Naturally, a group of experienced researchers to put this apparatus into operation and providing dosimetric information is essential. The GDN is considered one of these groups because, since the early 2000s [1,2,3] has developed Exposure Computational Models (ECMs) where the body is represented by a voxel phantom, the simulated radioactive sources emit photons and/or electrons, and the EGSnrc MC code [4] simulates the other tasks necessary in the assembly line of these evaluation systems. The ECMs already produced have thirteen algorithms that simulate external radioactive sources and a general algorithm for internal sources [5]. With them it is possible, for example, to obtain data for radiological protection. Figure 1 is the main window of the MCEsDataSid application, used in this work to read data from dosimetric simulations, organize them and present them in tables and graphs. The window background is an illustration of a typical. The 3D view is of the MASH (Male Adult meSH) phantom from DEN-UFPE, the font illustration is an image used in GDN publications and the third image was taken from the EGSnrc page. The texts that appear in this figure were translated into English, but the application window is originally in Portuguese. The same observation applies to Figures 3, 5 and 6 throughout the paper.

The developed phantoms [1,2,6,7,8,9] and part of the articles, dissertations and theses are available at http://dosimetrianumerica.org/ or may be requested from the authors. The phantoms were originally produced using voxel technology or they were voxelized with a developed method by the GDN group and implemented in the DIP software [10,11]. As this representation of the radiated geometry is a fundamental item in an ECM, it is necessary to have it available. The type of file most primary containing a stack of digital images is the RAW[1] binary. In 2009, Vieira and Lima [10] established the SGI (*Simulações Gráficas Interativas*/Interactive Graphic Simulations) type for the voxel phantoms of GDN. SGI is a binary format consisting of a header plus phantom data.

[1] RAW (raw) is a generic name for binary file formats containing digital images that store only data. Other information such as image dimensions is provided in additional text files.

Three integers of 4-byte for the column, row, and slice numbers of the parallelepiped containing the geometry form, in this order, the header of the SGI file; and the data are stored just like a RAW file.

To couple SGI phantom to EGSnrc, one more conversion is needed, also implemented in the DIP, which reads an SGI file and saves a text file with the DATA extension. All ECMs of the group used up to 2020 DATA files in coupling geometry to EGSnrc.

In 2021, the GDN developed, tested, and validated the new SID (*Sistema de Informações Dosimétricas*/Dosimetric Information System) format for text files intended to store voxel phantoms. Some articles are being produced to publicize the new tool. In addition to replacing the DATA format in ECMs, the SID can be read or written in GDN applications, which optimize the voxel phantom development.

Without exhausting the topic, this work presents the main ECMs that the GDN developed using voxel phantoms coupled with the EGS system. Both to prepare these MCEs and to execute them, obtain the results, organize them, and present them, the group developed several tools that are mentioned throughout the text. Some, such as the DIP, have specific publications and are used in courses given by the authors at their institutions.

Figure 1: *MCEsDataSid window with an illustration of an ECM formed by a phantom, a photon emitting source, and a MC code that simulates the transport of photons, and their interactions, and evaluates the energy deposited in the media of interest.*

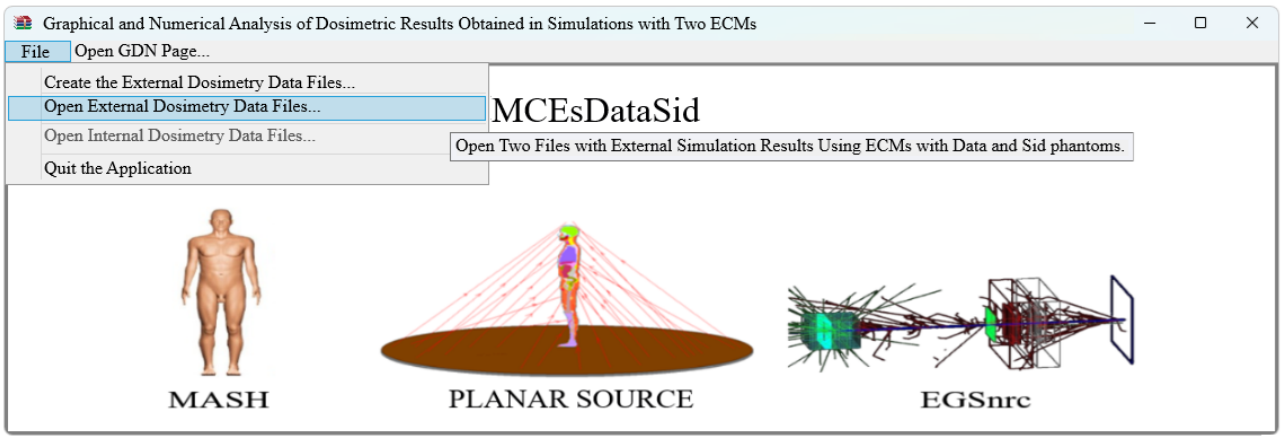

2. METHODOLOGY AND RESULTS

The materials used in this article are located in the Multiuser Laboratory of Numerical Dosimetry, Research Center, IFPE - campus Recife. The mentioned applications were developed in the Microsoft Visual Studio Community environment. Some illustrative images were produced in applications such as ImageJ, Paint, and Geany.

To place in time, the ECMs that GDN developed or any of its members collaborated in the development, the sequence of work was separated based on the primary images used in the production of the phantoms. At the end of this topic, a complete example of dosimetric evaluation performed by the group is presented and commented on.

2.1 Exposure Computational Models of with phantoms obtained from monochromatic images of the human body

The MAX was "born" from VOXTISS8 [12]. In 2005, Vieira and collaborators [13] published the FANTOMAS application, developed in API (Application Programming Interface) Windows C [14] to edit phantoms and save them in text files specially prepared for coupling to the MC EGS4 code [15]. With the application FANTOMAS, the VOXTISS8 data were read, resampled, reclassified, and adjusted to the reference man [16]. The MAX and the methods for evaluating the Equivalent Dose in the Red Bone Marrow and in the skin constituted the ECM MAX/EGS4 [1,3]. In 2004, Kramer et al [2] introduced the FAX/EGS4.

EGS4 code was replaced by EGSnrc in later ECMs. The FAX (Female Adult voXel) and the MAX phantoms were resampled with cubic voxels with 0.36 cm to 0.12 cm edges forming the FAX06-MAX06/EGSnrc ECMs, where the micro-CT method was implemented [17] for bone dosimetry [18]. This article is one of the chapters of the book edited by Xu and Eckerman, which synthesizes the golden age of voxel phantoms produced mainly from real images obtained by Computed Tomography (CT) or Magnetic Resonance Imaging (MRI). In the simulations, the algorithms of external source emitting photons with identifiers (IDs) 1, 2, 3, and 4 listed in Table 1 were used. Figure 2 shows views of the FAX, MAX, FAX06 and MAX06 phantoms obtained with the application Fiji/ImageJ (without skin, muscle, and soft tissue with tissue weighting factor (wT=0). The views of other phantoms shown in this article were produced in the same way. The

resampling effect that reduced the edges of the MAX and FAX voxels from 0.36 to 0.12 cm in the MAX06 and FAX06 versions can be seen in the images of the Figure 2.

Table 1: *Radioactive source algorithms implemented in GDN's ECMs.*

ID	Name
1	Parallel, AP (anteroposterior)
2	Parallel, PA (posteroanterior)
3	Parallel, LD (right side)
4	Parallel, LE (left side)
5	Parallel, Rotational
6	Punctual, AP (anteroposterior)
7	Punctual, PA (posteroanterior)
8	Punctual, LD (right side)
9	Punctual, LE (left side)
10	Punctual, Rotational
11	Isotropic in Space (4π)
12	Isotropic in the Upper Hemisphere (2π)
13	Parallel, AP (anteroposterior)
14	Internal Exposure

Figure 2: *3D views of FAX, MAX, FAX06, and MAX06 phantoms.*

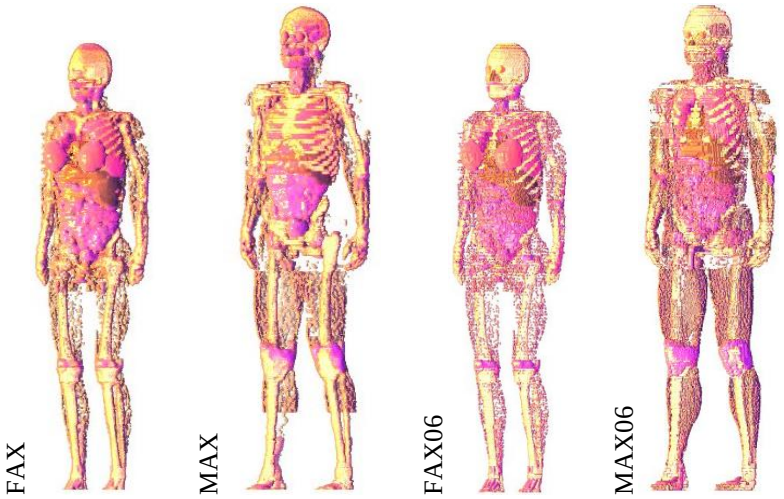

2.2 Exposure Computational Models with synthetic phantoms

One of the main problems in the development of voxel phantoms is the availability of primary whole-body data for computer simulations. Thus, the voxel technique, that is, the representation of images by bitmaps, was replaced by polygonal meshes. Synthetic phantoms were produced on the computer from 3D objects representing organs and tissues of the human body, obtained from specialized websites, usually produced by designers, based on information contained in anatomy books [8]. Thus, the possibility of modifying the geometry, which can be adjusted according to the purpose of the task, made it advantageous to produce synthetic phantoms. However, ECMs currently in use need the voxelized version. In 2020, Andrade and collaborators [11] published the mesh phantom voxelization method currently in use by the GDN.

In 2010, researchers from DEN-UFPE published the mesh phantoms in orthostatic position MASH (Male Adult meSH) and FASH (Female Adult meSH) [19,20]. In 2011, Cassola [21] constructed several mesh phantoms varying posture, mass, and height, including supine versions of the MASH and FASH. With MASH, MASH_SUP, FASH and FASH_SUP, and the algorithms with IDs 6, 7, 8 and 9 listed in Table 1, the dosimetric data for radiodiagnosis of CALDose_X (CALculation of Dose for X-ray diagnosis) were updated [17], an application originally developed in C++ and, from the sixth version, updated in C# with resources for graphical and numerical analysis of results selected by the user [22]. Figure 3 shows an example where, among the selected input data, are the exam type (abdomen) and the phantom (FASH_SUP).

So, it can be said that the most representative synthetic phantoms are MASH and FASH, used in several publications of the GDN group. To emphasize this point of view, it is enough to mention that the article [19] is one of the references of ICRP report 145 [25] on mesh phantoms. Figure 4 shows 3D views of these phantoms, whose ECMs resulting from the coupling to EGSnrc, named FSTA, FSUP, MSTA, and MSUP, are available on the DEN-UFPE website (http://www.caldose.org/). The fourteen radioactive source algorithms for dosimetry (thirteen for external and one for internal) [3,5], whose labels and names are listed in Table 1, complete these ECMs.

Figure 3: *Radiology dosimetry data displayed in the CALDose_X application.*

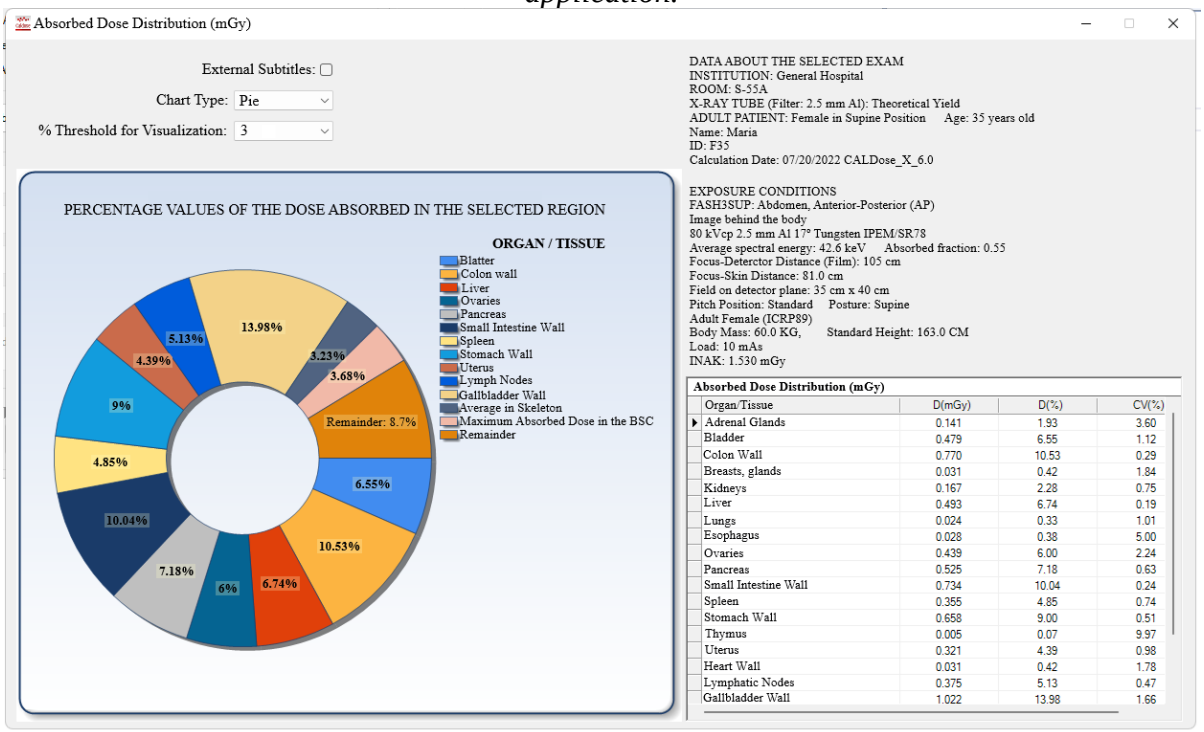

Figure 4: *3D views of the FASH, MASH, FASH_SUP, and MASH_SUP phantoms.*

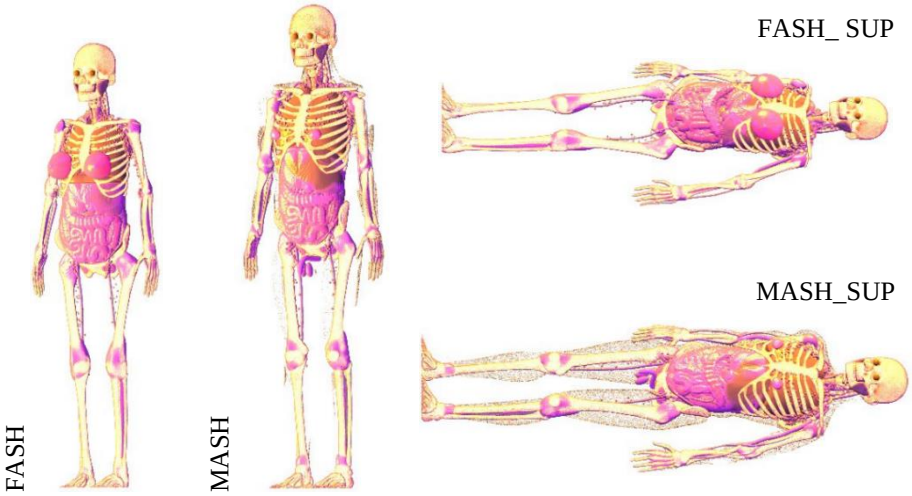

2.3 An example of external dosimetry

To illustrate all the necessary steps in a dosimetric evaluation, using the GDN methodology, the phantom MSTAFV17Sid was chosen. MSTAFV17 phantom is the acronym for the ECM presented in Vieira [5]. MSTA stands for Mash STAnding and FV is the acronym for the algorithm that, using MC techniques, estimates the frequency of trabecular voxels in the images of samples used by the μCT method [23] for dosimetric evaluations in bone tissues; And SID is the new acronym that the GDN uses both to designate the new ECMs developed from 2021 (the previous ones are identified in the group by DATA) and as an extension of the text file containing the geometry of the phantom coupled to EGSnrc. In DIP, it is possible to convert an SGI file into a SID.

To validate the ECMs SID, the MCEsDataSid Application was developed in C#, which reads the text files resulting from simulations of the ECMs DATA and SID, organizes and displays the produced data in tables and graphs, allowing the user to compare the two data distributions of voxels per organ as well as between the conversion coefficients (CCs) of the absorbed dose in the organs by incident air KERMA (Kinetic Energy Released per unit of MAss) (D/INAK). MSTAFV17Data and MSTAFV17Sid contain the same phantom (MASH) and the same FV algorithm (corresponding to the planar isotropic source in Table 1, used in environmental dosimetry simulations) [5].

As the initial state of the simulation, the FV algorithm produces a photon distribution on the surface of the phantom in an orthostatic position on the center of a flat disk, from which the photons originate at equally probable points. Both the voxel distribution per organ obtained at the end of the simulation and the D/INAK CCs prove that the SID methodology can replace the DATA in ECMs using voxel phantoms coupled to the EGSnrc, where the radioactive source emits photons and/or electrons. MCEsDataSid is one of the useful applications for dosimetrists that are available on the GDN page.

2.4 Simulation data organization

After the initial state, the photons go into the phantom, interact with atoms of this media, and are scattered or absorbed when they no longer have enough energy for new interactions (energy below a cut-off value), or leave the geometry. During the interactions, the numerical result of the

histories of all simulated photons is cumulatively computed in 3D, matrices that are the internal representation of the phantom. The data gathered in these matrices are organized and saved in text files at the end of the simulation. These are the files that need to be loaded through the MCEsDataSid Application menu item highlighted in Figure 1. If the user clicks on the "Open GDN Page..." menu, he/she will be able to obtain more information about the scientific production and activities of the group.

The data generated for this task were saved in the MSTAData.data and MSTASid.data files, which it must be loaded in the sequence DATA - SID, through the menu item highlighted in Figure 1. Then, the Application reads these data and displays them in tables in your window. The first table contains the output information about the two ECMs: ID, organ/tissue name, density (g/cm^3), voxel count, the difference between counts, CC D/INAK and variance coefficient, CV (%). In Santoro et al. [27], the CV statistical function is called relative error and quantifies the measurement dispersion of a quantity around the mean.

In addition to the features implemented in MCEsDataSid, the user can use some already established in the Windows environment, such as selecting, copying, and pasting data using the mouse and/or key combination. As an example, Table 2, with the information from the simulations, was selected and copied from the Application, and pasted into this text.

The information presented in Table 2 are in the files of the loaded ECMs. Note that there are input data such as the simulated particle type and its shear energy, but also the results obtained for simulation time, INAK/Fluency coefficient and, number of fluence photons, which in the case of the planar source, corresponds to the fraction of photons that would pass through a central sphere of radius 10 cm and 1 m from the plane, without the presence of the phantom [5]. These three results already show how similar the two ECMs are. It is worth noting that the computational time in the simulation with MSTAFV17Sid is slightly lower than that of MSTAFV17Data. This is due to the smaller number of mathematical and logic operations performed in the implementation of the SID methodology.

Still, in the main window of MCEsDataSid, the user can select a specific list of organs by checking their checkboxes. Four buttons in this window allow access to the graphical and numerical analysis of the selected collection.

Table 2: *Information about simulations with MSTAFV17Data and MSTAFV17Sid.*

PARAMETER	DATA	SID
Main Cubic Voxel Edge (cm)	0.12	0.12
Micro-CT Cubic Voxel Edge (cm)	0.0060	0.0060
Simulation Time (h)	8.23500	8.20333
Source Type / Projection	Isotropic / DISK	Isotropic / DISK
Maximum Initial Energy (keV)	100	100
Particle Type	Foton	Foton
No. of Media in the Fantoma	20	20
% Cellularity of Ribs	60.0	60.0
% Spine Cellularity	70.0	70.0
% Cellularity of Long Bones	25.0	25.0
% Cellularity of the Pelvis	48.0	48.0
% Cellularity of Skull/Jaws	38.0	38.0
INAK/Fluency in a Central Sphere (Gy*m²)	3.714E-13	3.714E-13
Number of Simulated Photons	500000000	500000000
No. of Fluency Photon	63142192	63107156
Cut Energy for Electrons (keV)	20	20
Cut Energy for Photons (keV)	2	2

2.5 Graphical and numerical analysis of voxel distributions

To exemplify how the application organizes and presents the results of the voxel distributions of the two ECMs, the fourteen most radiosensitive organs/tissues from ICRP 103 [26] ($wT \geq 0.01$) were selected. By clicking on the button “Distribution of Voxels...”, the new window shown in Figure 5 displays the graphical and numerical results of the selected collection. Note that the relationship coefficient between the two distributions is R=1, which means that they are statistically similar.

It can be seen in the last column of the table shown in Figure 5 that the difference between the number of voxels of the DATA simulation and that of the SID is 0, except for sponge bone tissues, which are segmented together in the MASH phantom and separated in the time of execution in EGSnrc, using the Micro-CT method [23]. In the table with all organs/tissues (main window), the number of voxels counted from spongy tissue as well as from the whole body is the same in both simulations. It is also shown in this table that the two more skin voxels in the SID distribution are missing from adipose tissue. Even with an insignificant amount of voxels, as they are organs/tissues segmented in MASH, it is necessary to verify in the future, with other phantoms, the origin of this exchange. The possibility of a coding error when reading the SID file in the EGSnrc user code is

already ruled out, because, if this were true, other segmented organ counts would give not null different from zero.

Figure 5: *Voxel distributions from major organs/tissues.*

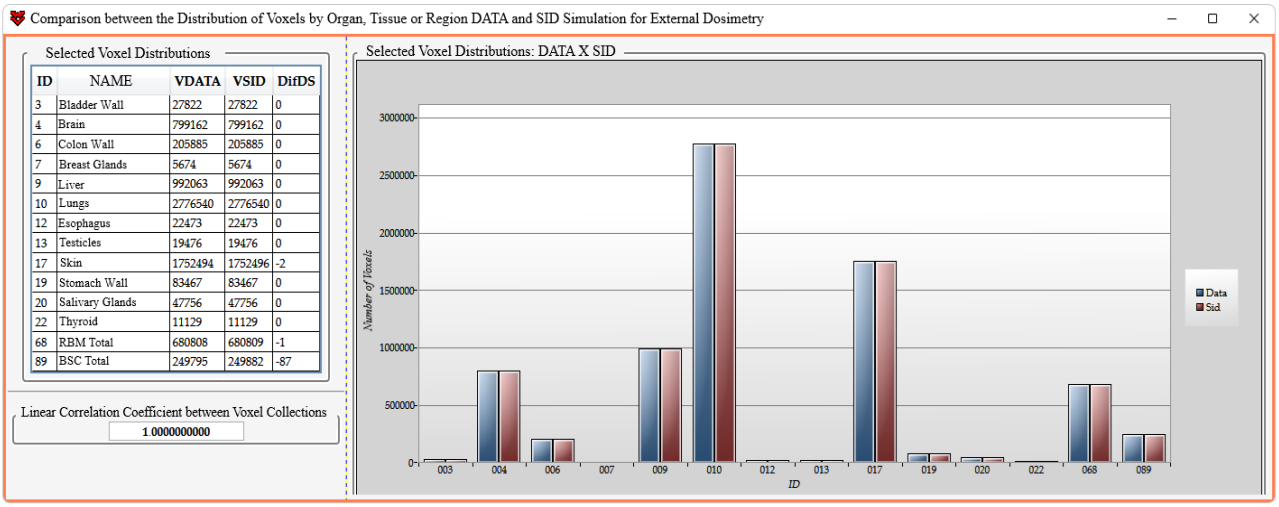

ID	NAME	VDATA	VSID	DifDS
3	Bladder Wall	27822	27822	0
4	Brain	799162	799162	0
6	Colon Wall	205885	205885	0
7	Breast Glands	5674	5674	0
9	Liver	992063	992063	0
10	Lungs	2776540	2776540	0
12	Esophagus	22473	22473	0
13	Testicles	19476	19476	0
17	Skin	1752494	1752496	-2
19	Stomach Wall	83467	83467	0
20	Salivary Glands	47756	47756	0
22	Thyroid	11129	11129	0
68	RBM Total	680808	680809	-1
89	BSC Total	249795	249882	-87

2.6 Graphical and numerical analysis of the conversion coefficients distributions absorbed dose by incident air KERMA

By selecting the most radiosensitive organs/tissues (except for the breast glands, where wT = 0.12 is attributed only to the female phantom) and clicking on the button “Distribution of D/INAK...”, it can be obtained the tables and the graphics arranged in a new window. Figure 6 shows the graph of CCs (D/INAK) of the most radiosensitive male organs/tissues from ICRP 103 for the two ECMs.

Figure 6: *CCs (D/INAK) and CVs of the most radiosensitive male organs.*

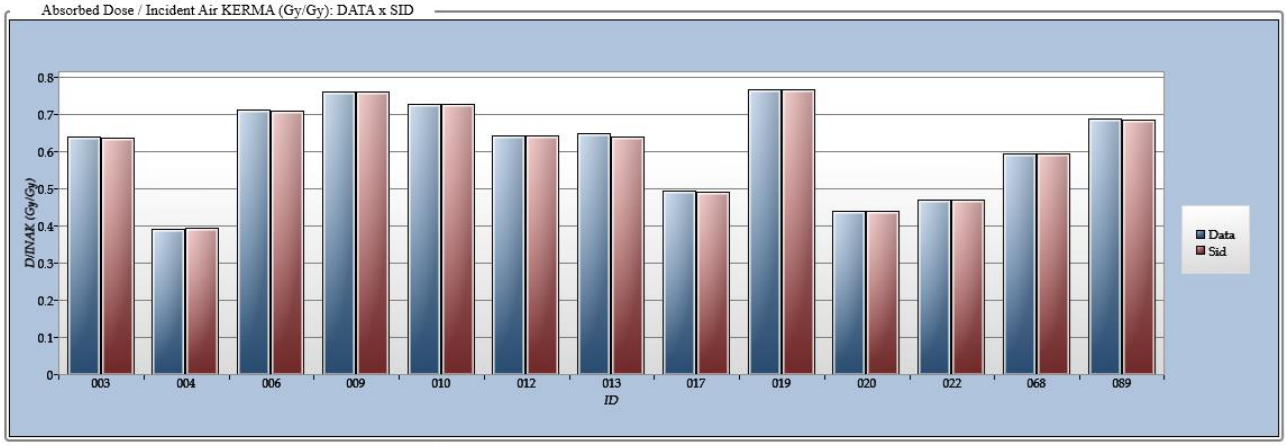

Tables 3, 4, and 5 complete the information transcribed into the text about the selected organ collection. As seen in Table 5, all male selected organs/tissues had CV < 0.30%, confirming not only that the number of photons used, 5E8 (Table 2), was adequate, regardless of the size and/or location of the organ tissue relative to the source, but also that the dosimetric results are statistically accurate. Table 4 shows that the mean values of the CVs are less than 0.20%. This table also shows R = 0.99982, which proves the similarity of dosimetric results with the precision of three decimal places (R = 1.000).

The small statistical fluctuation in the value of CVs is due to MC operations that occur throughout the history of a photon. Two MC simulations will produce different CVs. The important thing is that they are small enough for the simulation to be validated. One of the MC operations performed at runtime is the cumulative count of the fluence photons used to obtain the D/Fluency coefficients. Dividing the D/Fluency by the INAK/Fluency coefficient produces the D/INAK CCs printed in the output files. Table 3 shows the values of fluence photon numbers and INAK/Fluency, important parameters in dose normalization. The table also shows the male effective dose and cancer incidence risk and cancer mortality risk coefficients for the two simulations. All parameters shown in Table 3 for the simulations have a relative error below 0.35%.

Table 3: *Additional information obtained in the simulations.*

PARAMETERS	DATA	SID	ER (%)
INAK/Fluency in a Central Sphere (Gy*m²)	3.71E-13	3.71E-13	0
No. Photons of Fluency	63142192	63107156	0.0555
Full Body Average CC (Gy/Gy)	6.57E-01	6.55E-01	0.3058
E Male (Sv/Gy)	6.73E-01	6.72E-01	0.1559
RIC [(cases/1E5)/INAK (mGy)] 35 years	3.335	3.328	0.2099
RMC [(cases/1E5)/INAK (mGy)] 35 years	2.026	2.024	0.0987

Table 4: *Validation of MSTAFV17Sid against MSTAFV17Data.*

STATISTICAL FUNCTION	VALUE
Linear Correlation Coefficient for CCs	0.99982
Average Relative Error of CVsData (%)	0.17246
Average Relative Error of CVsSid (%)	0.17281

Table 5: *CCs D/INAK (Gy/Gy) SID DATE and the respective CVs (%) for the most radiosensitive male organs/tissues.*

ID	NAME	*D/INAK* DATA	*D/INAK* SID	*CV* DATA	*CV* SID
3	Bladder Wall	0.64284	0.63894	0.15	0.15
4	Brain	0.39444	0.39466	0.04	0.04
6	colon wall	0.71296	0.71165	0.05	0.05
9	Liver	0.76273	0.76296	0.03	0.03
10	Lungs	0.72997	0.72987	0.03	0.03
12	Esophagus	0.64419	0.64506	0.16	0.16
13	Testicles	0.65011	0.64329	0.18	0.18
17	Skin	0.49595	0.49259	0.02	0.02
19	stomach wall	0.77010	0.77020	0.08	0.08
20	Salivary glands	0.44138	0.44244	0.14	0.14
22	Thyroid	0.47092	0.47344	0.27	0.27
68	RBM total	0.59537	0.5947	0.03	0.03
89	Total BSC	0.68891	0.68787	0.05	0.05

3. CONCLUSIONS AND PERSPECTIVES

In this article, a brief review was carried out on ECMs composed of a voxel phantom coupled to the MC EGSnrc code for simulations in internal and external dosimetry. Some of the computational tools developed by the GDN were used. As a complete example, the results obtained from two ECMs were presented, whose main difference is in the way the voxel phantom used was written in the coupling to EGSnrc. In MSTAFV17Data, the writing has already been validated in publications until 2021; in MSTAFV17Sid, a new way to write a text file containing a phantom. This SID mode takes up less storage space, is more intuitive to read, can be used directly in other tasks such as viewing and editing, and reproduces the dosimetric results of the DATA version, as demonstrated by graphical and numerical analysis organized and displayed through DIP applications and MCEsDataSid.

The GDN has already started to organize a family of mesh phantoms by gender and age group, as suggested by ICRP 89 [16], to mainly evaluate the effective dose in accidental, medical, environmental, and industrial simulations. Figure 7 is formed by 3D views of phantoms already developed by the group: Children aged 5 and 10 years [24] MARIA (*Modelo Antropomórfico para dosimetria das Radiações Ionizantes em Adultas*/Anthropomorphic Model for Dosimetry of Ionizing Radiation in Adults) [6], SARA (*Simulador Antropomórfico para dosimetria das Radiações ionizantes em Adolescentes*/Anthropomorphic Simulator for dosimetry of Ionizing Radiation in Adolescents) [7,9], the MARTIN (Male Adult with Macro Circulation and Lymphatic

Vessels Phantom) [8], and the SAMUEL (*Simulador Antropomórfico Masculino para Dosimetria das Radiações Ionizantes em Adolescentes*/Anthropomorphic Male Simulator for Dosimetry of Ionizing Radiation in Adolescents) [9] are now ready for coupling and obtaining dosimetric data.

Figure 7: *GDN mesh phantoms to be used in future ECMs.*

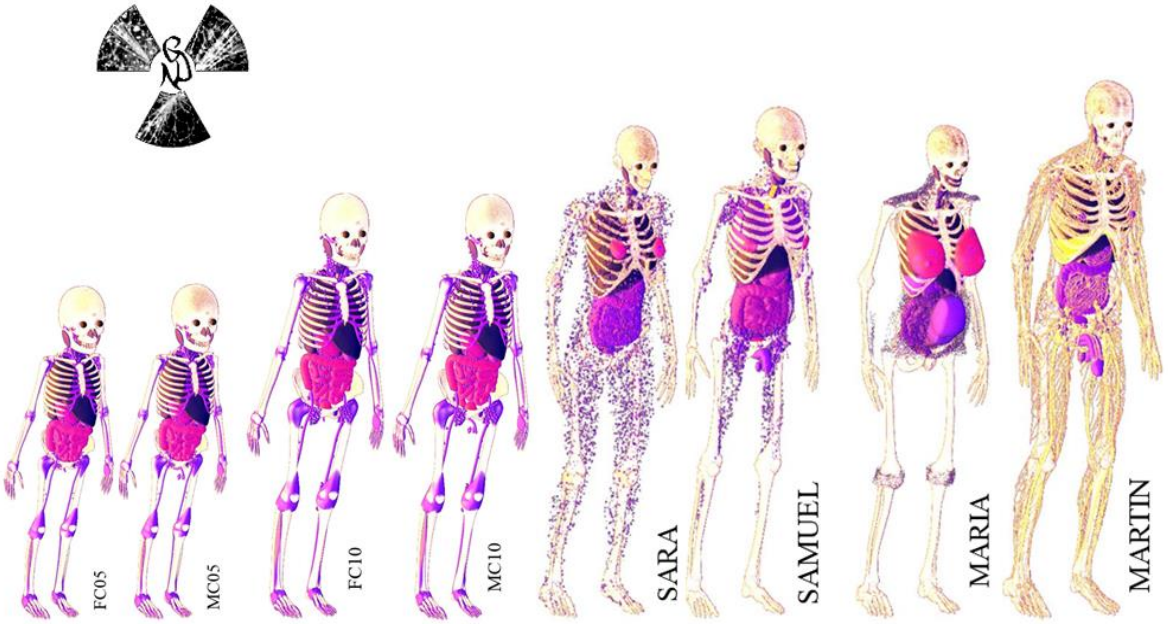

ACKNOWLEDGMENT

The authors are grateful to National Council for Scientific and Technological Development (CNPq), the Fundação de Amparo a Ciência e Tecnology de Pernambuco (FACEPE) and the Instituto Federal de Pernambuco (IFPE) - Campus Recife for the financial support of and the Centro Regional de Ciências Nucleares do Nordeste (CRCN-NE) for the computational infrastructure that allowed us to perform this article.

REFERENCES

[1] KRAMER, R., VIEIRA, J. W., KHOURY, H. J., LIMA, F. R. A., FUELLE, D., All About MAX: A Male Adult Voxel Phantom for Monte Carlo Calculations in the Area of Radiation Protection Dosimetry, Phys. Med. Biol., 48, 1239-1262, 2003.

[2] KRAMER, R., KHOURY, H. J., VIEIRA, J. W., LOUREIRO, E. C. M., LIMA, V. J. M., LIMA, F. R. A., HOFF, G., All About FAX: A Female Adult Voxel Phantom for Monte Carlo Calculation in Radiation Protection Dosimetry, Phys. Med. Biol., 49, 5203-5216, 2004.

[3] VIEIRA, J. W., Construção de um Modelo Computacional de Exposição para Cálculos Dosimétricos Utilizando o Código Monte Carlo EGS4 e Fantomas de Voxels, Tese de Doutorado em Tecnologias Energéticas e Nucleares, DEN-UFPE, Recife, Pernambuco, Brasil, 2004.

[4] KAWRAKOW, I., MAINEGRA-HING, E., ROGERS, D. W. O., TESSIER, F., WALTERS, B. R. B., The EGSnrc Code System: Monte Carlo Simulation of Electron and Photon Transport, NRCC Report PIRS-701, National Research Council of Canada, Ottawa, 2021.

[5] VIEIRA, J. W., MonteCarlo – Um Software para Uso em Avaliações Dosimétricas das Radiações Ionizantes, Tese para Progressão à Classe Titular do IFPE, Recife, Pernambuco, Brasil, 2017.

[6] CABRAL, M. O. M., Desenvolvimento de um Modelo Computacional de Exposição para Uso em Avaliações Dosimétricas em Gestantes, Dissertação de Mestrado em Tecnologias Energéticas e Nucleares, DEN-UFPE, Recife, Pernambuco, Brasil, 2015.

[7] SANTOS, P. N. C., Simulação de um Tratamento Radioterápico Crânio-Espinhal em um Fantoma de Voxel Infantil Utilizando Espaços de Fase Representativos de um Acelerador Linear, Dissertação de Mestrado em Tecnologias Energéticas e Nucleares, DEN-UFPE, Recife, Pernambuco, Brasil, 2016.

[8] ANDRADE, P. H. A., Construção e Voxelização de um Fantoma MESH Masculino Adulto com Macro Circulação e Vasos Linfáticos, Tese de Doutorado em Tecnologias Energéticas e Nucleares, DEN-UFPE, Recife, Pernambuco, Brasil, 2018.

[9] OLIVEIRA, E. S., Estimativa da Dose Efetiva em Fantomas de Voxel para Indivíduos de 15 Anos, Dissertação de Mestrado em Tecnologias Energéticas e Nucleares, DEN-UFPE, Recife, Pernambuco, Brasil, 2021.

[10] VIEIRA, J. W., LIMA, F. R. A., A Software to Digital Image Processing to Be Used in the Voxel Phantom Development, Cellular and Molecular Biology, 55, 16-22, 2009.

[11] ANDRADE, P. H. A., VIEIRA, J. W., OLIVEIRA, V. R. S., VELOSO, R. J. B., LIMA, F. R. A., Um Método para Voxelização de Geometrias 3D de Malhas, Brazilian Journal of Radiation Sciences, 08-01A, 01-10, 2020.

[12] ZUBAL I. G., The Yale Voxel Phantoms, http://noodle.med.yale.edu/zubal/, acessada em julho, 2022.

[13] VIEIRA, J. W., STOSIC, B., LIMA, F. R. A., KRAMER, R., SANTOS, A. M., LIMA, V. J. M., Um Software para Editar Fantomas de Voxels e Calcular Coeficientes de Conversão para a Proteção Radiológica, In: RADIO 2005, ABENDE, Rio de Janeiro, 2005.

[14] PETZOLD, C., Programming Windows, USA: Microsoft Press, 1999.

[15] NELSON, W. R., HIRAYAMA, H., ROGERS, D. W. O., The EGS4 Code System. Report SLAC-265, Stanford Linear Accelerator Center, Stanford University, Stanford, 1985.

[16] ICRP 89, Basic Anatomical and Physiological Data for Use in Radiological Protection Reference Values, International Commission on Radiological Protection, ICRP Publication 89, Pergamon Press, Oxford, 2003.

[17] KRAMER, R., KHOURY, H. J., VIEIRA, J. W., CALDose X – A Software Tool for the Assessment of Organ and Tissue Absorbed Doses, Effective Dose and Cancer Risks in Diagnostic Radiology. Phys. Med. Biol., 53, 6437-6659, 2008.

[18] KRAMER, R., KHOURY, H. J., VIEIRA, J. W., LIMA, V. J. M., LOUREIRO, E. C. M., HOFF, G., KAWRAKOW, I., The FAX06 and the MAX06 Computational Voxel Phantoms, In Xu, X. G., Eckerman, K. F. (ed.), Handbook of Anatomical Models for Radiation Dosimetry, Series in Medical Physics and Biomedical Engineering, CRC Press, 2010A.

[19] CASSOLA, V. F., LIMA, V. J. M., KRAMER, R., KHOURY, H. J., FASH and MASH: Female and Male Adult Human Phantoms Based on Polygon Mesh Surfaces: I. Development of the Anatomy, Phys. Med. Biol., 55, 133-162, 2010.

[20] KRAMER, R., CASSOLA, V. F., KHOURY, H. J., VIEIRA, J. W., LIMA, V. J. M., BROWN, K. R., FASH and MASH: Female and Male Adult Human Phantoms Based on Polygon Mesh Surfaces: II. Dosimetric Calculations, Phys. Med. Biol., 55, 163-189, 2010B.

[21] CASSOLA, V. F., Desenvolvimento de Fantomas Humanos Computacionais Usando Malhas Poligonais em Função da Postura, Massa e Altura, Tese de Doutorado em Tecnologias Energéticas e Nucleares, DEN-UFPE, Recife, Pernambuco, Brasil, 2011.

[22] VIEIRA, J. W., Implementação de Análise Gráfica e Numérica de Resultados Dosimétricos no Software CALDose_X, In: X Congreso Regional Latinoamericano IRPA de Protección y Seguridad Radiológica, Sociedad Argentina de Radioprotección, Buenos Aires, 2015.

[23] KRAMER, R., CASSOLA, V. F., VIEIRA, J. W., KHOURY, H. J., LIRA, C. A. B. O., BROWN, K. R., Skeletal Dosimetry Based on μCT Images of Trabecular Bone: Update and Comparisons, Phys. Med. Biol., 57, 3995-4021, 2012.

[24] LIMA, V. J. M., Desenvolvimento de Fantomas MESH Infantis, Morfologicamente Consistentes com a Anatomia Humana, para Uso em Dosimetria, Tese de Doutorado em Tecnologias Energéticas e Nucleares, DEN-UFPE, Recife, Pernambuco, Brasil, 2011.

[25] ICRP 145, Adult Mesh-Type Reference Computational Phantoms, ICRP Publication 145, Ann. ICRP 49 (3), 2020.

[26] ICRP 103, The 2007 Recommendations of the International Commission on Radiological Protection, ICRP Publication 103, Ann. ICRP 37 (2-4), 2007.

[27] SANTORO, A., MAHON, J. R., OLIVEIRA, J. U. C. L., MUNDIM FILHO, L. M., OGURI, V., SILVA, W. L. P., Estimativas e Erros em Experimentos de Física, Rio de Janeiro, ed. UFRJ, 2013.